Onset of "Hudson Strait" Heinrich events in the eastern North Atlantic at the end of the middle Pleistocene transition (~640 ka)?

David A. Hodell,[1,2] James E. T. Channell,[1] Jason H. Curtis,[1] Oscar E. Romero,[3] and Ursula Röhl[4]

Received 15 January 2008; revised 28 July 2008; accepted 10 September 2008; published 27 December 2008.

[1] Heinrich events are well documented for the last glaciation, but little is known about their occurrence in older glacial periods of the Pleistocene. Here we report scanning XRF and bulk carbonate $\delta^{18}O$ results from Integrated Ocean Drilling Program Site U1308 (reoccupation of Deep Sea Drilling Project Site 609) that are used to develop proxy records of ice-rafted detritus (IRD) for the last ~1.4 Ma. Ca/Sr is used as an indicator of IRD layers that are rich in detrital carbonate (i.e., Heinrich layers), whereas Si/Sr reflects layers that are poor in biogenic carbonate and relatively rich in detrital silicate minerals. A pronounced change occurred in the composition and frequency of IRD at ~640 ka during marine isotope stage (MIS) 16, coinciding with the end of the middle Pleistocene transition. At this time, "Hudson Strait" Heinrich layers suddenly appeared in the sedimentary record of Site U1308, and the dominant period of the Si/Sr proxy shifted from 41 ka prior to 640 ka to 100 ka afterward. The onset of Heinrich layers during MIS 16 represents either the initiation of surging of the Laurentide Ice Sheet (LIS) off Hudson Strait or the first time icebergs produced by this process survived the transport to Site U1308. We speculate that ice volume (i.e., thickness) and duration surpassed a critical threshold during MIS 16 and activated the dynamical processes responsible for LIS instability in the region of Hudson Strait. We also observe a strong coupling between IRD proxies and benthic $\delta^{13}C$ variation at Site U1308 throughout the Pleistocene, supporting a link between iceberg discharge and weakening of thermohaline circulation in the North Atlantic.

Citation: Hodell, D. A., J. E. T. Channell, J. H. Curtis, O. E. Romero, and U. Röhl (2008), Onset of ''Hudson Strait'' Heinrich events in the eastern North Atlantic at the end of the middle Pleistocene transition (~640 ka)?, *Paleoceanography*, *23*, PA4218, doi:10.1029/2008PA001591.

1. Introduction

[2] *Heinrich* [1988] first noted the occurrence of layers rich in ice-rafted detritus (IRD) and poor in foraminifera in sediment cores from the area of the Dreizack seamount in the eastern North Atlantic. These layers became the focus of much attention when *Broecker et al.* [1992] coined them "Heinrich events" and proposed that they were derived from massive discharges of ice from the Hudson Strait region of Canada. Much research has been focused on Heinrich events but, as pointed out by *Hemming* [2004], the definition of what constitutes a Heinrich event differs widely among researchers and study regions. We adopt the definition of *Bond et al.* [1999] that the diagnostic feature of Heinrich events is the presence of detrital carbonate (limestone and dolomite) derived from lower Paleozoic basins of northern Canada [*Broecker et al.*, 1992; *Andrews*, 1998; *Bond et al.*, 1999; *Hemming*, 2004]. Heinrich events are also marked by their high lithic-to-foraminifer ratio and increased relative abundance of the polar planktic foraminifer *Neogloboquadrina pachyderma* sinistral [*Heinrich*, 1988].

[3] Six Heinrich events were originally recognized for the last glacial period and labeled "H1" through "H6" [*Bond et al.*, 1992]. Two additional events have been proposed (e.g., H0 and H5a [*Andrews et al.*, 1995; *Bond and Lotti*, 1995; *Stoner et al.*, 1996; *Rashid et al.*, 2003a]), but these events are rarely recorded outside the Labrador Sea and western North Atlantic. *Hemming* [2004] defined a subgroup of four Heinrich layers (specifically H1, H2, H4, and H5) that were described as "cemented marls" in German lithologic core descriptions, and share a set of characteristics that are consistent with an origin from Hudson Strait [*Hemming et al.*, 1998]. This subgroup is referred to as "Hudson Strait" (HS) Heinrich events [*Hemming*, 2004]. The HS Heinrich layers are distinguished from other events such as H3 and H6, which display a lower flux of IRD in the central and eastern North Atlantic [*McManus et al.*, 1998; *Hemming*, 2004] and possibly contain significant amounts of detritus derived from European and/or Greenland sources [*Grousset et al.*, 1993; *Gwiazda et al.*, 1996; *Snoeckx et al.*, 1999].

[4] Many studies of North Atlantic detrital layer stratigraphy have focused on the IRD belt of the central North Atlantic [*Bond et al.*, 1992, 1993, 1999; *Grousset et al.*,

[1]Department of Geological Sciences, University of Florida, Gainesville, Florida, USA.
[2]Now at Godwin Laboratory for Paleoclimate Research, Department of Earth Sciences, University of Cambridge, Cambridge, UK.
[3]Instituto Andaluz de Ciencias de la Tierra, Universidad de Granada, Granada, Spain.
[4]Center for Marine Environmental Research, University of Bremen, Bremen, Germany.

0883-8305/08/2008PA001591$12.00

1993; *Bond and Lotti*, 1995; *Snoeckx et al.*, 1999], whereas others have documented detrital events in more ice proximal locations such as the Labrador Sea [e.g., *Andrews and Tedesco*, 1992; *Hillaire-Marcel et al.*, 1994; *Stoner et al.*, 1995, 1996, 2000; *Hiscott et al.*, 2001; *Rashid et al.*, 2003a, 2003b], the Irminger Basin off east Greenland [*Elliot et al.*, 1998; *van Kreveld et al.*, 1996], and the Porcupine Seabight off SW Ireland [*Scourse et al.*, 2000; *Walden et al.*, 2006; *Peck et al.*, 2007]. Although Heinrich events have been well studied for the last glacial cycle, less is known about their occurrence in older glacial periods of the Pleistocene [*Hiscott et al.*, 2001; *Hemming*, 2004]. Such studies have been hampered by the availability of long continuous cores with high sedimentation rates from the North Atlantic IRD belt.

[5] Here we address several questions concerning the Pleistocene history of HS Heinrich events using proxy data from Integrated Ocean Drilling Program (IODP) Site U1308 (reoccupation of Deep Sea Drilling Project (DSDP) Site 609): When did Heinrich layers first appear in the sedimentary record of the central North Atlantic? Were they restricted to the "100-ka world" when continental ice volume was large or are they also found in the "41-ka world" when ice sheets were reduced in size? What is the relationship between Heinrich events and the Mid Pleistocene Transition (MPT)? Is there a critical ice volume (thickness) threshold or duration of glacial conditions needed to produce Heinrich events? What was the relationship between Heinrich and other IRD events and thermohaline circulation during the Pleistocene?

2. Materials and Methods

2.1. IODP Site U1308

[6] DSDP Site 609 has featured prominently in studies of millennial-scale climate variability of the last glacial cycle, including the recognition of Heinrich events and their correlation to Greenland Ice cores [*Bond et al.*, 1992, 1993, 1999; *McManus et al.*, 1994; *Bond and Lotti*, 1995]. DSDP Site 609 is located near the center of the North Atlantic IRD belt that trends west-southwest along latitude 46 to 50°N and marks the band of maximum iceberg melting and IRD deposition during the last glaciation (Figure 1 [*Ruddiman*, 1977]). During IODP Exp 303, DSDP Site 609 was reoccupied and a complete composite section was obtained at Site U1308 to 239 m composite depth (mcd) [*Expedition 303 Scientists*, 2006]. The apparent continuity of the recovered section at Site U1308 represents a significant improvement on the section recovered 25 years ago at DSDP Site 609 that preceded the shipboard construction of composite sections. The water depth of 3427 m places the site within lower North Atlantic Deep Water (NADW) in the open Atlantic out of the direct path of overflows from the Norwegian-Greenland Sea.

[7] Here we report data from the upper ~100 mcd at Site U1308. In this interval, the shipboard composite section was modified postcruise because a few core sections used in the shipboard splice showed evidence of disturbance during postcruise sampling (Table 1).

2.2. Stable Isotopes

[8] Stable isotopes were measured on the benthic foraminifer *Cibicidoides wuellerstorfi* and/or *Cibicidoides kullenbergi* at a sample spacing of 2 cm for the upper 100 mcd of Site U1308. Specimens were picked from the >212-μm size fraction, and one to five individuals were used for analysis. Foraminifer tests were soaked in ~15% H_2O_2 for 30 min to remove organic matter. The tests were then rinsed with methanol and sonically cleaned to remove fine-grained particles. The methanol was removed with a syringe, and samples were dried in an oven at 50°C for 24 h. The foraminifer tests were crushed and between 20 to 60 μg of calcite was loaded into glass reaction vessels, and reacted with three drops of H_3PO_4 (specific gravity = 1.92) using a Finnigan MAT Kiel III carbonate preparation device. Isotope ratios were measured online by a Finnigan MAT 252 mass spectrometer. Analytical precision was estimated to be ±0.07 for $\delta^{18}O$ and ±0.03 for $\delta^{13}C$ by measuring eight standards (NBS-19) with each set of 38 samples.

2.3. Magnetic Susceptibility

[9] Whole cores were logged aboard the JOIDES Resolution using a GEOTEK multisensor core logger. Shipboard logging was carried out at 5-cm resolution. Sediment bulk density was estimated by gamma ray attenuation (GRA) and magnetic susceptibility was measured using the 4.5-cm Bartington loop sensor. We also took u-channel samples (plastic containers with a 2 × 2 cm square cross section and a typical length of 150 cm [*Tauxe et al.*, 1983]) from the center of split core sections along the spliced composite section and remeasured magnetic susceptibility every 1 cm using a custom-built instrument in the Paleomagnetic Laboratory at the University of Florida [*Thomas et al.*, 2003; *Channell et al.*, 2008]. The 3.3-cm square coil of this instrument has a smaller response function (~3-cm half peak width) than the 4.5-cm Bartington loop sensor (~10-cm half peak width) used aboard ship, thereby providing greater spatial resolution. The susceptibility meter was zeroed before each section was analyzed and a drift correction applied between the beginning and end of each section analyzed.

2.4. XRF Analysis

[10] Using an Avaatech XRF core scanner at the University of Bremen, we measured the full suite of elements between Al and Ba in the upper 100 mcd of the spliced composite section of Site U1308. The split core surface was carefully scraped cleaned and covered with a 4 μm thin SPEXCertiPrep Ultralene foil to avoid contamination and prevent desiccation [*Richter et al.*, 2006]. Each section was scanned twice: once at 0.2 milliamps (mA) and 10 kilovolts (kV) to measure Al to Fe (including Si and Ca) and another at 1 mA and 50 kV to measure Rb through Ba (including Sr). A 1-cm^2 area of the core surface was irradiated with X rays using 30 s count time. XRF data were collected every 1 cm along the spliced section of Site U1308, resulting in ~10,000 measurements with an average temporal resolution of less than 200 years. Elemental ratios (Ca/Sr and Si/Sr) were calculated using the corrected counts for each of the respective elements.

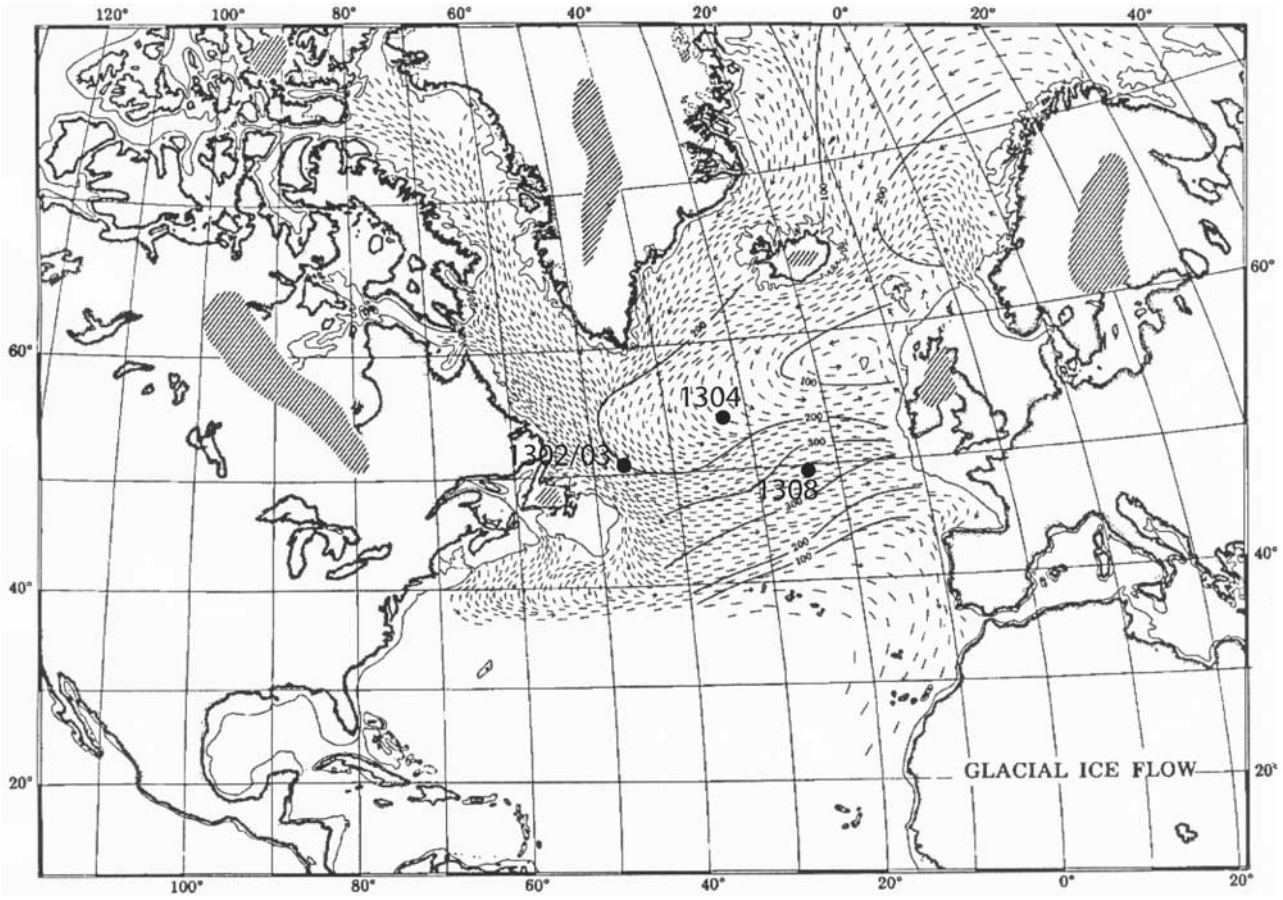

Figure 1. Position of IODP Sites U1302/03, U1304, and U1308 relative to IRD accumulation for the last glaciation (modified after *Ruddiman* [1977]). Arrows represent mean paths of distributions of ice-rafted debris during glacial periods inferred by *Ruddiman* [1977].

Table 1. Modified Sampling Splice Tie Points, Site U1308

								Corresponding Splice Tie Point							
Site	Hole	Core	Type	Section	Interval (cm)	Depth (mbsf)	Depth (mcd)	Site	Hole	Core	Type	Section	Interval (cm)	Depth (mbsf)	Depth (mcd)
1308	C	1	H	2	144	2.94	2.94	1308	E	1	H	2	12	1.62	2.94
1308	E	1	H	7	10	9.1	10.42	1308	C	2	H	3	6	7.46	10.42
1308	C	2	H	5	106	11.46	14.42	1308	E	2	H	2	12	11.12	14.42
1308	E	2	H	6	126	18.26	21.56	1308	C	3	H	2	138	16.78	21.56
1308	C	3	H	6	40	21.8	26.58	1308	E	3	H	2	58	21.08	26.58
1308	E	3	H	4	106	24.56	30.06	1308	B	4	H	3	16	26.16	30.06
1308	B	4	H	6	28	30.78	34.68	1308	A	4	H	2	92	30.02	34.68
1308	A	4	H	5	142	35.02	39.68	1308	C	5	H	1	142	34.32	39.68
1308	C	5	H	5	72	39.62	44.98	1308	A	5	H	2	86	39.46	44.98
1308	A	5	H	6	76	45.34	50.86	1308	C	6	H	1	104	43.44	50.86
1308	C	6	H	5	144	49.81	57.23	1308	F	6	H	3	4	49.97	57.23
1308	F	6	H	6	126	55.69	62.95	1308	B	7	H	3	34	54.84	62.95
1308	B	7	H	6	68	59.68	67.79	1308	A	7	H	2	132	58.92	67.79
1308	A	7	H	3	142	60.52	69.39	1308	F	7	H	2	124	59.74	69.39
1308	F	7	H	5	136	64.36	74.01	1308	C	8	H	2	94	63.84	74.01
1308	C	8	H	5	66	68.06	78.23	1308	A	8	H	3	104	69.64	78.23
1308	A	8	H	6	74	73.84	82.41	1308	B	9	H	2	75.5	72.76	82.41
1308	B	9	H	5	76.8	77.27	86.94	1308	E	9	H	2	6	80.56	86.94
1308	E	9	H	5	28.5	85.29	91.63	1308	F	9	H	3	5.1	79.05	91.63
1308	F	9	H	6	119.1	84.69	97.29	1308	A	10	H	2	107	87.17	97.29
1308	A	10	H	6	98.7	93.09	103.21								

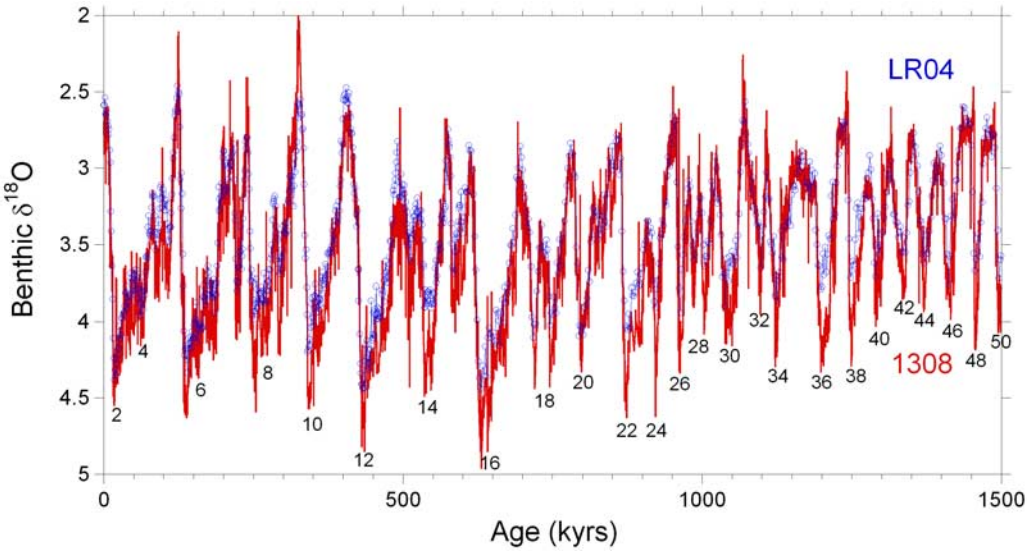

Figure 2. Benthic oxygen isotope record of Site U1308 (red) compared to the stacked oxygen isotope record of *Lisiecki and Raymo* [2005] (LR04; blue).

[11] We verified the scanning XRF data from the split-core sediment surface by analyzing dried, homogenized powders of 50 samples from Sites U1308 using a conventional XRF analyzer (Spectro Xepos EDPXRF) [*Wien et al.*, 2005]. This method has been shown to be effective for calibrating scanning XRF data [*Tjallingii et al.*, 2007]. Approximately 10 cc of sediment were sampled at 50 depths at Site U1308, freeze dried, ground, and ~4 g of sediment was loosely packed into plastic sample holders with bottoms consisting of 4-μm XRF foil. The samples selected included a range of Ca, Si and Sr values and ratios and included Heinrich events 1 through 6 (see auxiliary material).[1]

2.5. Bulk Carbonate $\delta^{18}O$

[12] For bulk stable isotope analysis, ~1 cc of sediment was dried in an oven at 50°C and the sample was ground to a homogenous powder. Bulk samples were reacted in a VG Isocarb carbonate preparation device with H_3PO_4 at 90°C for 15 min which is sufficient to react both calcite and dolomite completely. Oxygen and carbon isotopes of evolved CO_2 gas were measured using a Micromass PRISM Series II mass spectrometer. Analytical precision (1 standard deviation) was estimated to be ±0.06‰ for $\delta^{18}O$ and ±0.04‰ for $\delta^{13}C$ by measuring standards (NBS-19, n = 85) with each set of 36 samples.

2.6. Age Model

[13] The age model of Site U1308 was constructed using radiocarbon dates and oxygen isotope stratigraphy (Figure 2 and Table 2). Back to 35 ka, radiocarbon dates from DSDP Site 609 [*Bond et al.*, 1993] were transferred to the mcd scale of Site U1308 by correlating gray scale signals obtained from core photographs (see auxiliary material). From 35 to 60 ka, the benthic $\delta^{18}O$ record was correlated to MD95–2042 thereby utilizing the SFCP04 time scale [*Shackleton et al.*, 2004] that has also been applied to the Greenland ice cores [*Svensson et al.*, 2006]. Prior to 60 ka, the benthic $\delta^{18}O$ record was correlated to the stacked $\delta^{18}O$ record of *Lisiecki and Raymo* [2005]. Every isotopic stage between marine isotope stage (MIS) 1 and 50 is identifiable, supporting the completeness of the composite section at Site U1308. Benthic foraminifera are scarce at the transition of MIS 10 to MIS 9 and, consequently, the position of Termination IV is not well constrained. Sedimentation rates average ~7 cm/ka in the upper 100 mcd but interval sedimentation rates vary considerably.

3. Results

3.1. IRD Proxies

[14] Core scanning XRF data from Site U1308 were compared with existing petrologic counts of ice-rafted detritus (IRD) from DSDP Site 609 [*Bond et al.*, 1992, 1999; *Bond and Lotti*, 1995] to identify proxies for monitoring various components of IRD. Ca and Sr are highly correlated and covary over glacial-to-interglacial cycles of the Pleistocene, reflecting variations in biogenic carbonate content of the sediment (Figure 3). An exception occurs during the Heinrich layers H1, H2, H4 and H5, however, when Ca increases but Sr remains relatively low (Figure 4). These HS Heinrich layers also display high Ca/Sr when measured on dried, homogenized samples using a conventional XRF instrument (see auxiliary material). The greatest Ca/Sr ratios in the core occur when detrital carbonate content is high and biogenic carbonate is low. This relationship occurs because biogenic calcite precipitated by coccoliths and foraminifera has a greater Sr concentration than inorganically precipitated calcite or dolomite owing to the fact that the Sr partition coefficient (K_{DSr}) for biogenic

[1]Auxiliary materials are available in the HTML. doi:10.1029/2008PA001591.

Table 2. Depth-Age Points Used to Construct Chronology for Site U1308[a]

Depth (mcd)	Age (ka)	Calibration
0.68	13.8	^{14}C
0.69	13.0	^{14}C
0.74	13.0	^{14}C
0.80	14.4	^{14}C
0.82	15.6	^{14}C
0.87	15.4	^{14}C
0.92	17.4	^{14}C
0.95	19.1	^{14}C
0.99	19.5	^{14}C
1.08	20.1	^{14}C
1.18	22.5	^{14}C
1.23	23.7	^{14}C
1.25	25.3	^{14}C
1.29	25.6	^{14}C
1.34	26.9	^{14}C
1.59	30.4	^{14}C
1.63	31.7	^{14}C
1.69	31.4	^{14}C
1.76	34.6	^{14}C
1.90	35.3	SFCP04
2.01	36.1	SFCP04
2.80	40.1	SFCP04
3.10	42.7	SFCP04
3.50	48.0	SFCP04
4.14	56.0	SFCP04
4.50	62	LR04
5.24	72	LR04
5.90	86	LR04
6.22	93	LR04
7.06	104	LR04
8.75	127	LR04
9.17	136	LR04
11.54	191	LR04
12.42	201	LR04
13.65	220	LR04
15.32	243	LR04
18.06	281	LR04
18.74	292	LR04
21.42	325	LR04
21.85	341	LR04
24.73	392	LR04
27.40	431	LR04
29.06	475	LR04
32.68	513	LR04
34.92	534	LR04
37.56	580	LR04
38.58	596	LR04
39.88	622	LR04
43.72	690	LR04
47.24	726	LR04
48.72	746	LR04
51.14	788	LR04
52.58	814	LR04
56.41	866	LR04
58.52	902	LR04
60.20	922	LR04
64.37	964	LR04
65.71	978	LR04
65.97	984	LR04
67.73	998	LR04
68.05	1004	LR04
70.41	1032	LR04
72.07	1058	LR04
72.77	1070	LR04
77.25	1098	LR04
78.25	1108	LR04
79.99	1126	LR04
80.75	1132	LR04
86.10	1200	LR04
87.20	1218	LR04
87.56	1222	LR04
89.90	1250	LR04
91.86	1290	LR04
94.38	1316	LR04
96.62	1340	LR04
98.20	1354	LR04
100.68	1372	LR04
102.20	1398	LR04
102.96	1406	LR04
103.71	1412	LR04
103.96	1418	LR04
104.67	1426	LR04
105.63	1442	LR04
106.31	1448	LR04
106.46	1456	LR04
108.71	1488	LR04
109.04	1496	LR04
109.99	1510	LR04

[a]Radiocarbon dates from *Bond et al.* [1993]. SFCP04, *Shackleton et al.* [2004]; LR04, *Lisiecki and Raymo* [2005].

calcite is much greater than that for inorganic calcite and dolomite.

[15] At Site U1308, four distinct Ca/Sr peaks occurred during the last glacial period corresponding to Heinrich layers 1, 2, 4, and 5 at Site 609 (Figures 5a and 5b). These four layers were originally described as "cemented marls" [see *Hemming*, 2004] and are also marked by increases in density and magnetic susceptibility (Figure 5c). Magnetic susceptibility has been shown previously to serve as a proxy for IRD deposition in North Atlantic sediments [*Robinson et al.*, 1995; *Stoner et al.*, 1996; *Stoner and Andrews*, 1999; *Kissel*, 2005]. H3 and H6 are not associated with peaks in Ca/Sr and are marked by low carbonate content at Site U1308. The low carbonate of H3 and H6 may be a result of dissolution and/or low carbonate productivity [*Gwiazda et al.*, 1996]. Although *Bond et al.* [1992] reported small increases in percent detrital carbonate associated with H3 and H6 at Site 609 (Figure 5a), the amount is too small to be detected by Ca/Sr measured by scanning or conventional XRF. *Ji et al.* [2008] found dolomite to be present in H3 and H6 at Site U1308, but concentrations were barely above background levels as measured by XRD and only ~3% dolomite estimated by FTIR. In contrast, H1, H2, H4 and H5 have >15% dolomite [*Ji et al.*, 2008]. In cores from the Labrador Sea, however, H3 and H6 are associated with increases in detrital carbonate believed to be sourced from Hudson Strait [*Hillaire-Marcel et al.*, 1994; *Stoner et al.*, 1998; *Rashid et al.*, 2003a, 2003b]. If H3 and H6 were also caused by surging of Hudson Strait ice, then most ice bergs may have melted in the western Atlantic with low fluxes to the central and eastern parts of the IRD belt [*Gwiazda et al.*, 1996].

[16] Bulk carbonate δ^{18}O at Site U1308 reflects the relative proportion of biogenic and detrital carbonate and resembles the lithic-to-foraminifer ratio at Site 609 (Figures 5d and 5e [*Hodell and Curtis*, 2008]). All six Heinrich layers are marked by decreases in bulk carbonate δ^{18}O; however, the decrease is less for H3 and H6 than for other

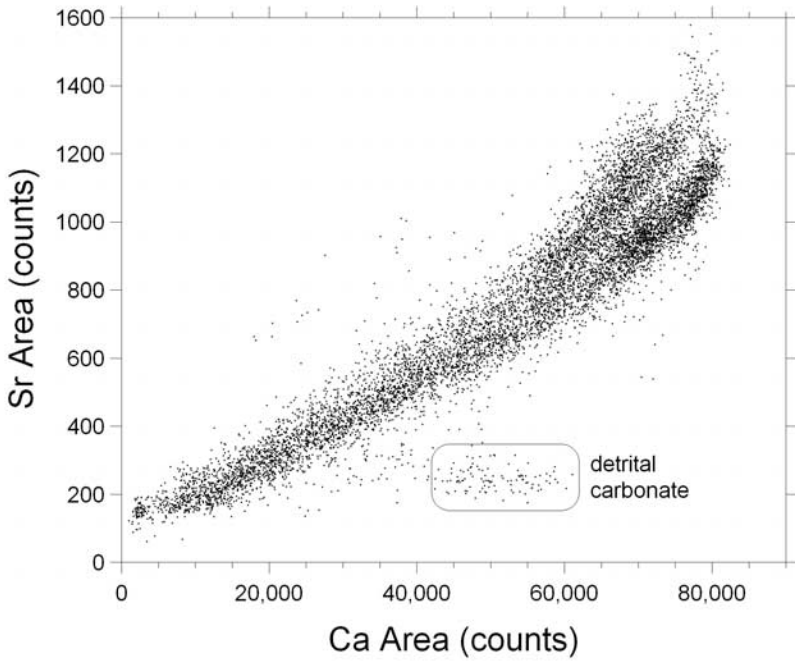

Figure 3. Ca versus Sr for the top 100 mcd at Site U1308. Detrital carbonate events are marked by high Ca and low Sr as indicated by area enclosed by oval.

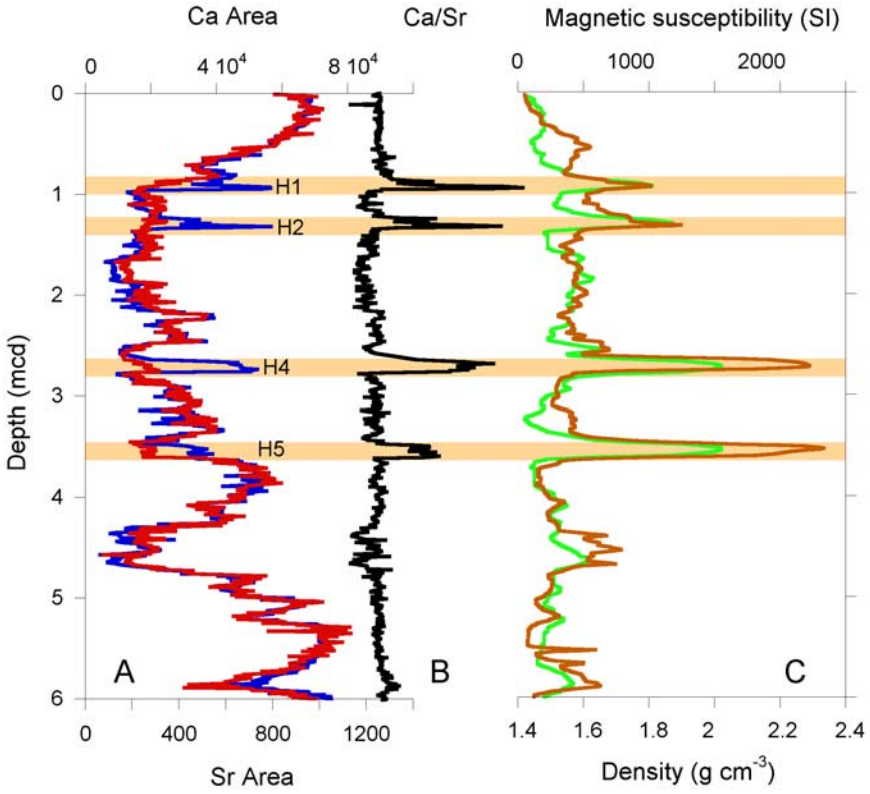

Figure 4. (a) Peak areas for Ca (blue) and Sr (red) measured by scanning XRF for the upper 6 mcd at Site U1308, (b) ratio of Ca to Sr, and (c) magnetic susceptibility (green) and density (brown). Positions of Heinrich events 1, 2, 4 and 5, are highlighted by orange shading.

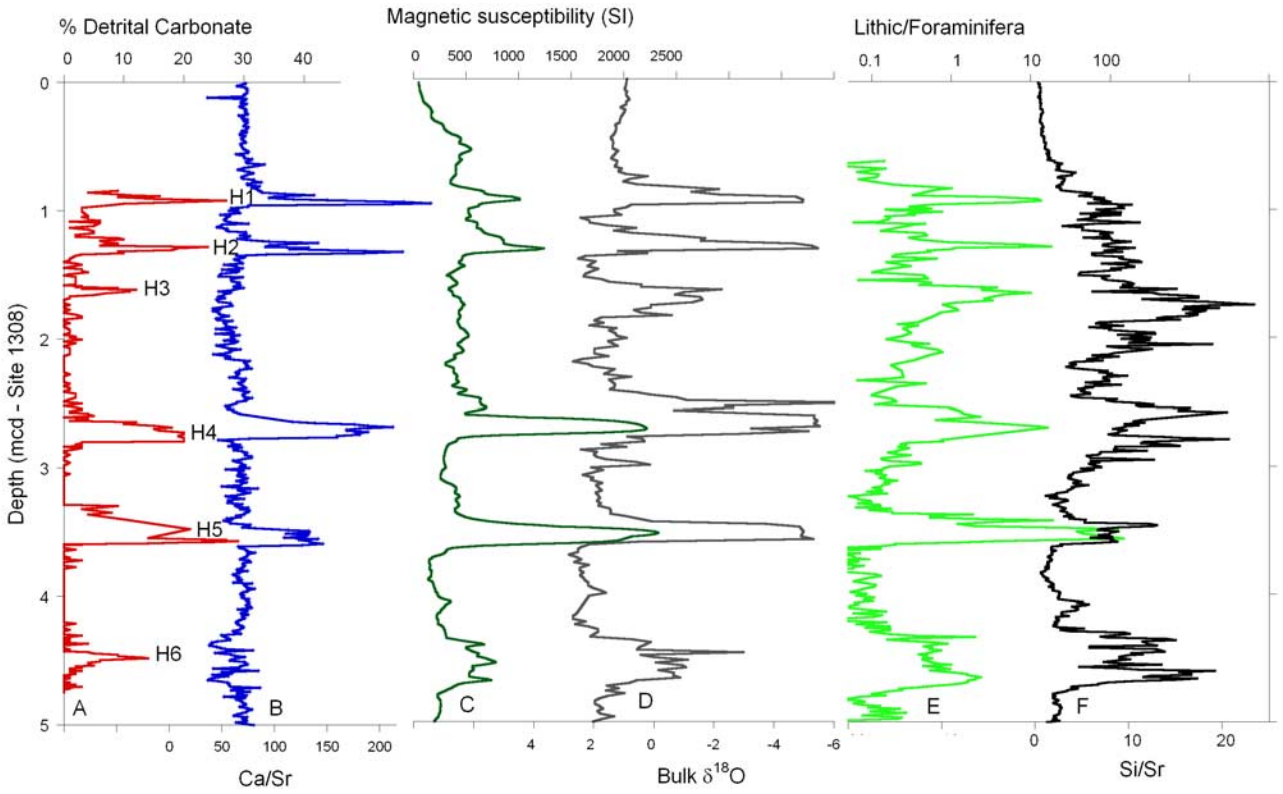

Figure 5. Comparison of (a) percent detrital carbonate (red) at Site 609 [*Bond et al.*, 1992] with (b) Ca/Sr, (c) magnetic susceptibility, (d) bulk carbonate $\delta^{18}O$, (e) the ratio of lithics to foraminifera (green) at Site 609 [*Bond et al.*, 1992], and (f) Si/Sr at Site U1308.

Heinrich events (Figure 5d). During HS Heinrich layers 1, 2, 4 and 5, bulk $\delta^{18}O$ decreases to approximately −5‰ and values are indistinguishable from those of detrital carbonate grains in the coarse fraction [*Hodell and Curtis*, 2008]. During H3 and H6, $\delta^{18}O$ decreases to only about −2‰. No change in bulk $\delta^{18}O$ is associated with H0 or H5a.

[17] The ratio of Si to Sr (Si/Sr) at Site U1308 resembles the lithic-to-foraminifer ratio at Site 609 [*Bond et al.*, 1992] (Figure 5f). We use Si/Sr and bulk carbonate $\delta^{18}O$ to recognize layers in cores from Site U1308 that are poor in biogenic carbonate (i.e., low Sr and Ca) and relatively rich in detrital silicate minerals (e.g., quartz, feldspar, etc.). Peaks in Si/Sr tend to co-occur with lows in bulk carbonate $\delta^{18}O$, and may represent either decreased biogenic carbonate productivity and/or increased delivery of IRD rich in silicate minerals.

3.2. Downcore Variations in IRD Proxies

[18] The criteria used to recognize HS (“cemented marl–type”) Heinrich layers in the older record at Site U1308 includes a concomitant increase in Ca/Sr, density and magnetic susceptibility, and a decrease of bulk carbonate $\delta^{18}O$ to <−5‰ as observed during H1, 2, 4 and 5 during the last glaciation (Figures 5 and 6a). IRD events that are poor in detrital carbonate and rich in silicate minerals are identified by peaks in Si/Sr, low Ca/Sr, and decreases in bulk $\delta^{18}O$ reaching about −2‰ (Figures 5 and 6a). In contrast to the last glaciation, MIS 6 shows no evidence for any HS detrital carbonate layers, but two peaks in Si/Sr and lows in bulk $\delta^{18}O$ are observed (Figure 6b). An IRD event occurs at Termination II and coincides with H11 described elsewhere in North Atlantic cores [*Heinrich*, 1988; *McManus et al.*, 1994; *Chapman and Shackleton*, 1998; *Lototskaya and Ganssen*, 1999; *Oppo et al.*, 2001, 2006], whereas the other occurs at ∼150 ka. MIS 8 contains three HS Heinrich layers including one at Termination III (Figure 6c). A Si-rich IRD event precedes the Heinrich layer at Termination III and another occurs at ∼273 ka. A large peak in Ca/Sr occurs on Termination IV although the exact position of the deglaciation is difficult to locate because of a gap in the benthic isotope record at the transition from MIS 10 to 9 (Figure 6d). MIS 12 contains one HS Heinrich layer centered on Termination V, and multiple peaks in Si/Sr and lows in bulk $\delta^{18}O$ occur throughout the glaciation (Figure 6e). No detrital carbonate layers occur in MIS 14 which was a relatively weak glaciation. Two HS Heinrich layers occurred during MIS 16, including one associated with Termination VI (Figure 6f). In addition, there were many peaks in Si/Sr and lows in bulk $\delta^{18}O$ during MIS 16. No detrital carbonate layers occur in any of the glacial periods older than MIS 16 during the past 1.4 Ma (Figure 7).

[19] A distinct change in the frequency and amplitude of IRD proxies occurred at ∼640 ka in MIS 16. The frequency

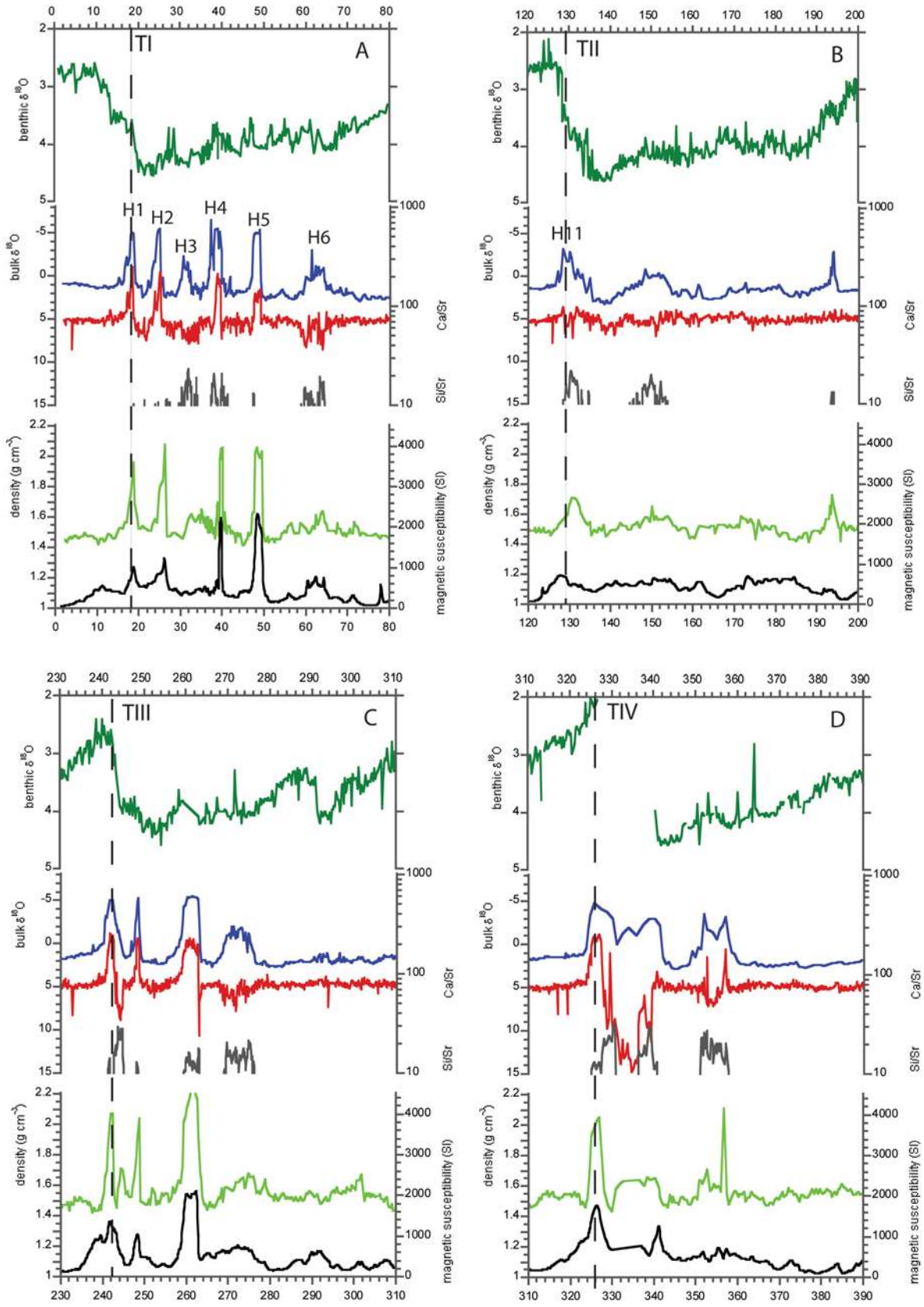
TI
A
TII
B
TIII
C
TIV
D
H1
H2
H3
H4
H5
H6
benthic δ18O
bulk δ18O
Ca/Sr
Si/Sr
density (g cm-3)
magnetic susceptibility (SI)

Figure 6

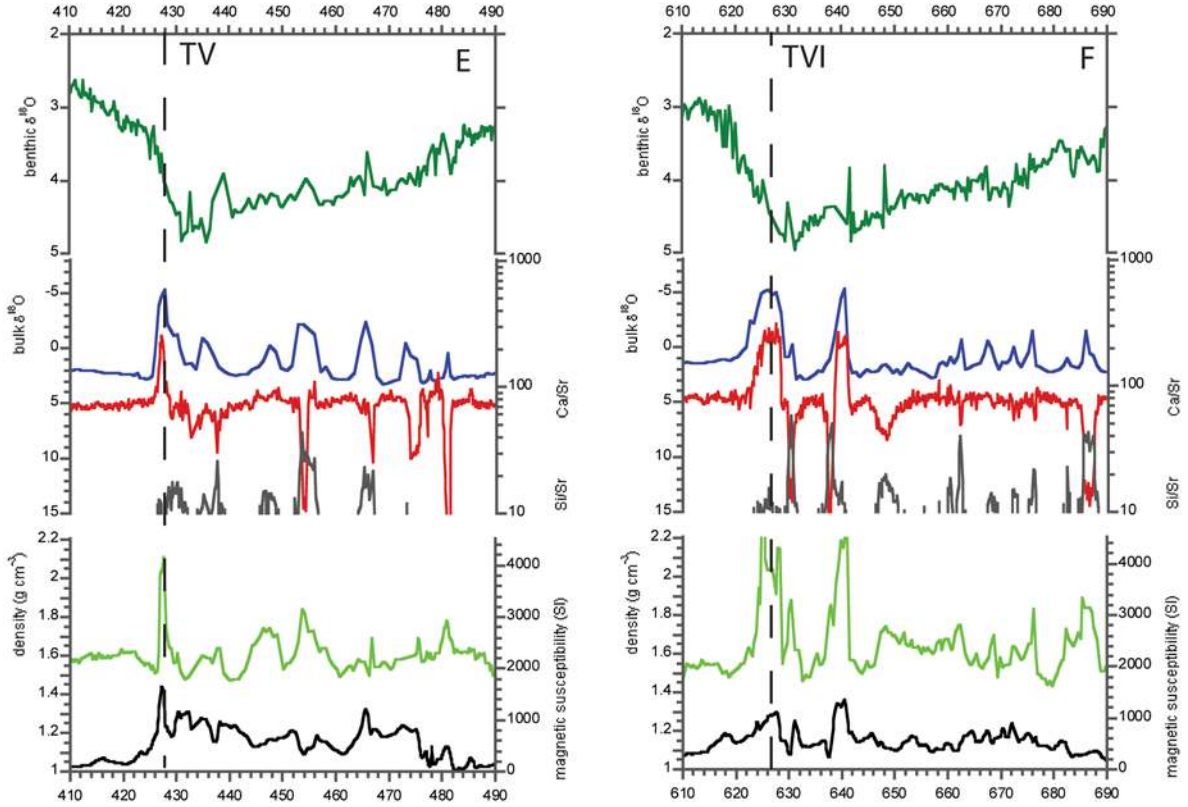

Figure 6. (continued)

of magnetic susceptibility and density variations diminishes (Figures 7a and 7b) and the amplitude increases associated with the first occurrence of detrital carbonate layers (Figure 7c). The amplitude of Si/Sr variations decrease and Si/Sr peaks become less frequent after MIS 16 (Figure 7d). Bulk carbonate $\delta^{18}O$ also shows a change from more frequent lows with minimum values of −2‰ prior to 640 ka, to less frequent lows after 640 ka with minimum values reaching −5‰ during HS Heinrich layers (Figure 7e).

4. Discussion

4.1. HS Heinrich Events in Older Glacial Periods

[20] We follow the lead of *Hemming* [2004] and distinguish "cemented marl–type" Heinrich events that originate from Hudson Strait (HS) from other types of Heinrich and IRD events whose origins are more ambiguous. HS Heinrich events were not limited to the last glaciation at Site U1308 and the number of layers varied from 4 (MIS2–4), 3 (MIS 8), 2 (MIS 16 and 10), to 1 (MIS 12) (Figures 6 and 7). During each of the glacial periods, HS Heinrich layers are found toward the latter part of the glacial cycle and almost always on glacial terminations (Figures 6 and 7). We refer to these latter events as TIREs (terminal ice rafting events) following the terminology of *Venz et al.* [1999]. No large detrital carbonate IRD events are recognized in glacial MIS 6 and 14 or any of the glacial stages prior to MIS 16 (Figure 7). Although MIS 6 contains no HS Heinrich layers at Site U1308 (Figures 6b and 7), two Si-rich IRD events are indicated by peaks in Si/Sr and lows in bulk carbonate $\delta^{18}O$ (Figure 6b). An IRD event occurred on Termination II (Figure 6b), coinciding with Heinrich event 11 (i.e., TIRE II) found elsewhere in the North Atlantic [*McManus et al.*, 1994, 1998; *Chapman and Shackleton*, 1999; *Lototskaya and Ganssen*, 1999; *Oppo et al.*, 2001, 2006], but it was not rich in detrital carbonate.

[21] No detrital-carbonate-rich Heinrich layers are found at Site U1308 during MIS 6 yet benthic $\delta^{18}O$ values indicate that ice volume was as great as other glacial periods containing HS Heinrich events. In core MD95–2025 in the Labrador Sea, to the south of Orphan Knoll, *Hiscott et al.* [2001] reported a number of minor peaks in ice rafting during MIS 6, but no Heinrich layers were recognized there either. At Site U1302/02, located on Orphan Knoll, *Romero and Hodell* [2007] reported several peaks in Ca/Sr during MIS 6 that may represent detrital carbonate layers, although it is uncertain whether these events were ice rafted or represent fine-grained sediment lofting from turbiditic overflows from the North Atlantic Mid-Ocean Channel (NAMOC) [see

Figure 6. Benthic (dark green) and bulk carbonate (blue) $\delta^{18}O$, Ca/Sr (red), and Si/Sr (gray) along with density (light green) and magnetic susceptibility (black) for 80-ka time periods during MIS (a) 2–4, (b) 6, (c) 8, (d) 10, (e) 12, and (f) 16. Ca/Sr and Si/Sr are plotted on a log scale with a lower limit of 10 to emphasize the peaks in Si/Sr only. Dashed vertical line and roman numerals refer to the termination of each glacial stage.

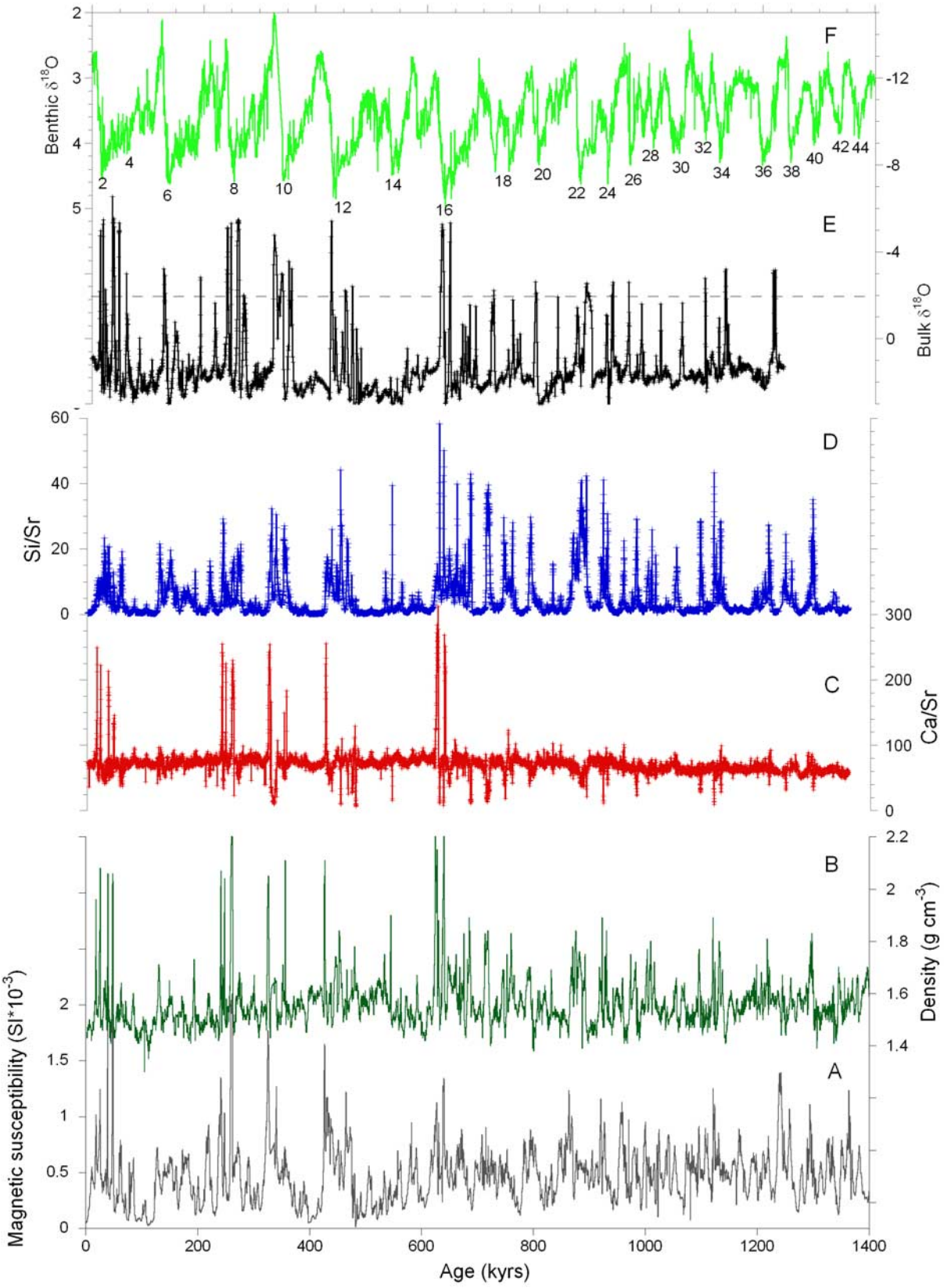

Figure 7. (a) Magnetic susceptibility, (b) density, (c) Ca/Sr, (d) Si/Sr, (e) bulk carbonate δ^{18}O, and (f) benthic δ^{18}O for the last 1.4 Ma at Site U1308. Glacial marine isotope stages are numbered. Detrital carbonate layers, marked by peaks in Ca/Sr, first occurred at 640 ka during MIS 16.

Hillaire-Marcel et al., 1994; *Hesse et al.*, 2004]. If icebergs were produced off Hudson Strait during MIS 6, they may have dropped most of their IRD in the western North Atlantic before reaching Site U1308. The accumulation of ice-rafted detritus in the North Atlantic approximately follows the northern limit of the zone of zero wind stress curl, and is associated with the melting of icebergs along the southern boundary of the polar waters [*Grousset et al.*, 1993]. Therefore, circulation changes associated with a more northerly position of the polar front during MIS 6 compared to the last glaciation would have influenced the position of maximum iceberg melting [*Calvo et al.*, 2001; *de Abreu et al.*, 2003]. In the western Mediterranean, *Martrat et al.* [2004, 2007] found fewer abrupt events during MIS 6 compared with the last glaciation suggesting that the nature of millennial-scale variability may have been different.

[22] In each of the glacial periods where HS Heinrich layers occur at Site 1308, they are found toward the latter part of the glacial cycle and nearly always at glacial terminations (Figure 7). *Marshall and Clark* [2002] found that a substantial fraction (60 to 80%) of the Laurentide ice sheet was frozen to the bed for the first 75 ka of a 120-ka simulation of the last glacial cycle using an ice sheet model driven by Greenland temperature. The fraction of warm-based ice increased substantially in the latter part of the glacial cycle as the ice sheet thickened and expanded, thereby increasing basal flow resulting in thinning the ice sheet interior and calving at marine margins. The flux of icebergs and IRD would be expected to increase as the glacial cycle progresses. Once a substantial fraction of the bed reaches the melting point, the ice sheet becomes predisposed to events that may trigger a dynamic response and result in the production of a Heinrich event. The occurrence of ice rafting events on terminations (TIREs) is probably related to strong feedback processes that hasten the demise of the ice sheet during deglaciation [*Alley and Clark*, 1999].

[23] Peaks in Si/Sr are generally coincident with low bulk δ^{18}O, and represent layers that are relatively rich in detrital silicate minerals (e.g., quartz, feldspar, etc.) and poor in detrital and biogenic carbonate. Some Si/Sr peaks may not represent increases in the flux of IRD, but rather reflect a relative increase in detrital silicates when biogenic carbonate production was reduced. Millennial-scale peaks in Si/Sr are more common than Ca/Sr peaks and represent a different source and/or glaciological process than HS Heinrich layers (Figure 7). Si-rich IRD events may be derived from multiple ice sheets and contain substantial contributions from European ice sheets. Peaks in Si/Sr and Ca/Sr may also represent different glaciological processes. *Marshall and Koutnik* [2006] suggested that a distinction be made between more frequent millennial-scale IRD fluctuations (reflected by Si/Sr) and infrequent HS Heinrich events (reflected by Ca/Sr). Non-Heinrich IRD events may reflect climate-driven changes in the mass balance of ice sheets as a result of advance and retreat of the grounding line from sources throughout the circum-Atlantic. In contrast, the much larger sediment fluxes containing detrital carbonate associated with HS Heinrich events represent episodes of internal dynamical instability of the LIS in the region of Hudson Strait.

4.2. Heinrich Events and the Middle Pleistocene Transition

[24] During the MPT, the average climate state evolved toward generally colder conditions with larger ice sheets (see *Clark et al.* [2006] for discussion of ice volume and deep water temperature changes across the MPT). Benthic δ^{18}O increased from ~942 to 892 ka followed by an abrupt increase in the amplitude of the 100-ka cycle at ~640 ka [*Mudelsee and Stattegger*, 1997; *Mudelsee and Schulz*, 1997]. Only after ~700 ka, however, does the benthic δ^{18}O signal exhibit maximum glaciations with its strongest power at a quasiperiodicity of ~100 ka [*Clark et al.*, 2006].

[25] The MPT represents a major change in the response of the climate system from a linear system dominated by 41-ka power to a nonlinear system dominated by 100-ka power. Several explanations for the MPT invoke a change in the size and dynamics of northern hemisphere ice sheets [*Berger and Jansen*, 1994; *Clark and Pollard*, 1998; *Clark et al.*, 2006]. A pronounced change occurred in the composition and frequency of IRD at ~640 ka during MIS 16, coinciding with the end of the MPT. The first detrital carbonate layer appeared in the stratigraphic record of Site U1308 at ~640 ka, coinciding with the establishment of the dominance of the 100-ka cycle in the benthic δ^{18}O signal (Figures 8a and 8b). Furthermore, Si/Sr ratios show a switch from dominantly 41-ka power before 650 ka to 100-ka power thereafter (Figures 8c and 8d).

[26] An important question is whether HS Heinrich events were produced during the "41-ka world" prior to 640 ka or not. If Heinrich events result from instability associated with excess ice, then they would not be expected to occur in the 41-ka world when the LIS was thinner. *Clark and Pollard* [1998] suggested that the LIS was thin because of a widespread basal deforming sediment layer with low friction that limited the thickness of the ice sheet. Alternatively, Heinrich events may have been produced in glacial periods prior to 640 ka but not preserved at Site U1308 because of warmer North Atlantic sea surface temperatures. We discuss both iceberg production and survivability as possible explanations for the abrupt appearance of Heinrich layers in the Site U1308 record at 640 ka.

[27] The glaciological processes responsible for Heinrich events may have first become active at 640 ka because MIS 16 represents the first of the "super" glaciations of the Pleistocene when benthic δ^{18}O values exceed 4.5‰ and excess ice was stored in Northern Hemisphere ice sheets (Figure 2). A variety of mechanisms have been proposed to explain Heinrich events that call upon excess ice (i.e., thickness) and/or low temperatures. One is the "binge-purge" model that purports that as an ice sheet thickens, it acts as an insulator trapping geothermal and frictional heat at its base (the thicker the ice sheet, the greater the insulation). Once the pressure melting point is reached, the melted unconsolidated base acts as a slip plane resulting in surging [*MacAyeal*, 1993a, 1993b; *Alley and MacAyeal*, 1994]. MIS 16 may have been the first time that the LIS grew thick enough to reach the pressure melting point in the region of Hudson Strait, thereby producing the first HS Heinrich events. An alternative model for Heinrich events has been proposed whereby ice advances across Hudson

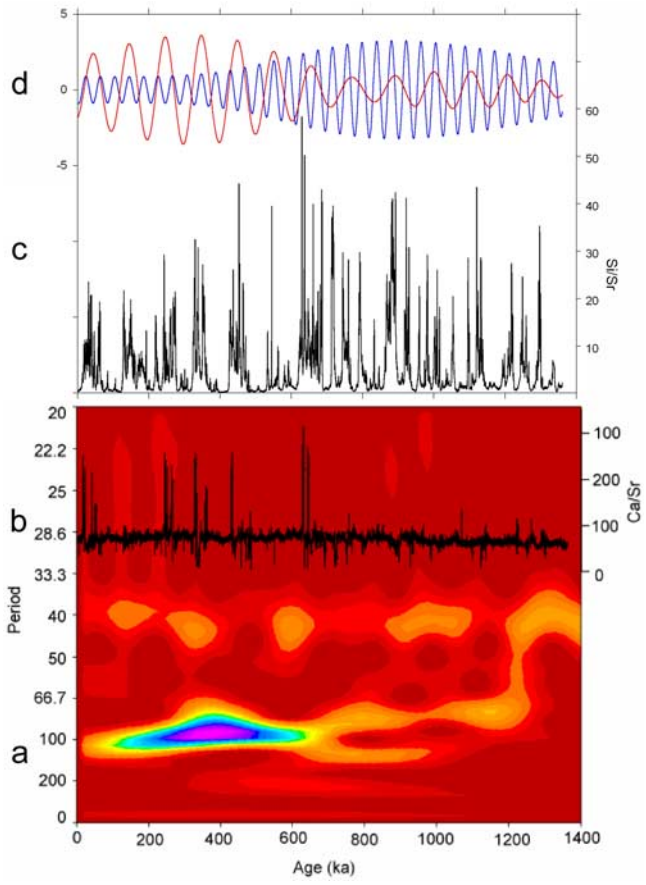

Figure 8. (a) Wavelet analysis of benthic $\delta^{18}O$ variation, (b) Ca/Sr, (c) Si/Sr, and (d) the 41-ka (blue) and 100-ka (red) filtered components of the Si/Sr signal at Site U1308. Time series analysis of the lognormalized Si/Sr data showed significant (0.95 confidence limit) power at 100 and 41 ka. Note that the onset of IRD deposition rich in detrital carbonate (Ca/Sr peaks) coincided with the increase in the amplitude of the 100-ka cycle.

Strait and the eastern basin until it reaches the Labrador Sea where it forms a fringing ice shelf. IRD is incorporated into the ice by basal freeze-on especially in the eastern basin, and climate change can trigger ice shelf collapse and rapid dispersal of IRD [*Hulbe*, 1997; *Hulbe et al.*, 2004; *Clark et al.*, 2007]. In this case, the extreme cold conditions needed to form fringing ice shelves along the eastern Canadian seaboard may have first developed in MIS 16.

[28] Are Heinrich events related to an ice volume (thickness) and/or temperature threshold? The benthic $\delta^{18}O$ record reflects both temperature and ice volume changes (Figure 2), and Heinrich events 4 and 5 occurred in MIS 3 when benthic $\delta^{18}O$ was 3.8‰. If Heinrich events were simply related to an ice volume threshold, then we would expect them to occur in glacial periods with similar benthic $\delta^{18}O$ values during the 41-ka world but they do not at Site U1308. We note, however, that relative ice volume and deep water temperature contributions to benthic $\delta^{18}O$ may have changed through the Pleistocene as well as the mean $\delta^{18}O$ of the ice sheets [*Clark et al.*, 2006]. Heinrich events only occur toward the end of glacial cycles, so the duration of glaciation may also play a role. Glacial periods have become progressively longer during the last 1.5 Ma (Figure 9). At Site U1308, HS Heinrich events only occur in those glacial periods that exceed ~50 ka in duration (with the exception of MIS 6 where they are absent). The observation that Heinrich events are favored by lengthy glaciations may be related to the increasing fraction of the ice sheet underlain by warm based ice as the glacial cycle progresses, culminating at the glacial termination [*Marshall and Clark*, 2002; *Clarke et al.*, 2005]. A long duration (e.g., tens of thousands of years) may be required for ice sheets to become sufficiently thick to reach the basal melting point and initiate fast-flow processes (e.g., surges). As more of the underlying LIS reaches the melting point, the ice sheet becomes more susceptible to events that may trigger a dynamic response, thereby resulting in a Heinrich event.

[29] Alternatively, the appearance of detrital carbonate layers at 640 ka at Site U1308 may be a signal of iceberg survivability rather than production. Variations in sea surface conditions or atmospheric circulation may have affected the survivability or drift direction of icebergs and the position of the IRD belt relative to Site U1308 (Figure 1). Few records of North Atlantic sea surface temperature exist across the MPR. At DSDP Site 607 (41°N), SST cooled at the onset of the MPT and reached minimum values by 900 ka [*Ruddiman et al.*, 1989; *Clark et al.*, 2006]. SSTs then began to rise from 900 to 600 ka. Although cooling did occur across the MPT, minimum SST values preceded the first occurrence of Heinrich events by ~250 ka. At ODP Sites 980 (55°N) and 984 (61°N), faunal data indicate that the Arctic front was located farther south prior to 660 ka and

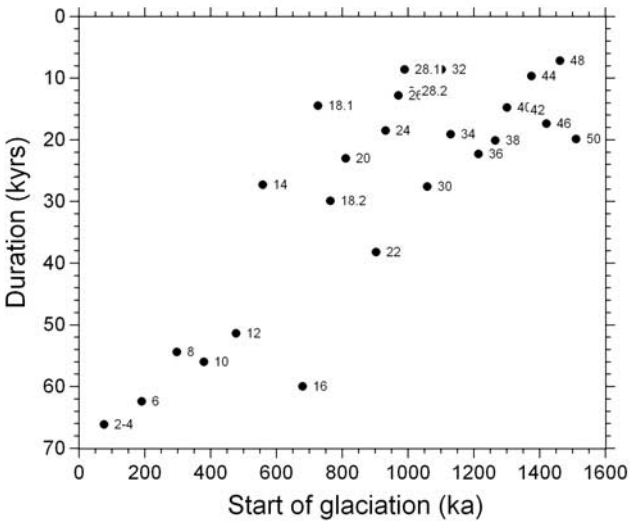

Figure 9. Duration of glacial periods as defined by when benthic $\delta^{18}O$ exceeds 3.5‰ versus start time of the glacial period. The duration of glacial periods increased significantly across the MPR when HS Heinrich events began to appear in the Site U1308 record. As the length of glacial conditions increases, the fraction of the LIS underlain by warm-based ice also increases, thereby rendering the ice sheet more susceptible to events that may trigger a Heinrich event.

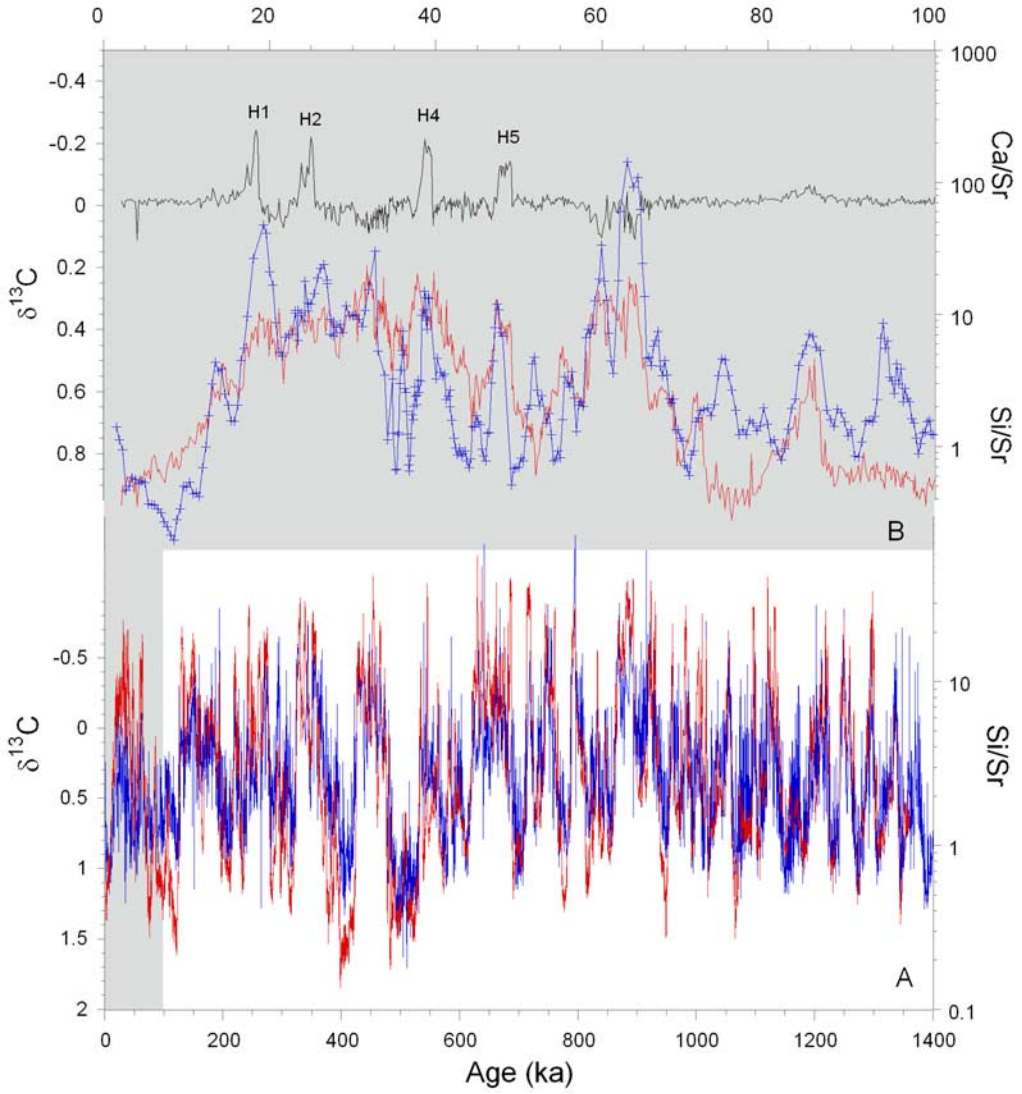

Figure 10. (a) Benthic $\delta^{13}C$ (blue) and Si/Sr (red) for the last 1.4 Ma. Peaks in Si/Sr correlate with minima in benthic $\delta^{13}C$. (b) Comparison of Si/Sr (red) with five-point running mean of benthic $\delta^{13}C$ (blue) for the last 100 ka. Heinrich events are identified by peaks in Ca/Sr (black).

moved northward afterward [*Wright and Flower*, 2002]. This observation also suggests that glacial North Atlantic SST conditions were cold enough prior to 660 ka for icebergs to survive the transport to Site 1308 if they were produced off Hudson Strait. Smaller ice sheets prior to the MPT may have impacted atmospheric circulation such that iceberg from the LIS could have taken a more northerly route than after the MPT. If this was the case, then we might expect to find HS Heinrich events in more northerly sites, such as Site 1304 (Figure 1), prior to 640 ka. Studies of additional sites are needed to confirm whether HS Heinrich events were limited to the past 640 ka.

[30] The Si/Sr values indicate that IRD was delivered to Site U1308 during glacial periods prior to 640 ka but it was composed principally of silicate minerals and lacked significant amounts of detrital carbonate (Figure 7). The appearance of detrital carbonate in the IRD of Site U1308 at 640 ka represents a change in provenance that included the introduction of material from Hudson Strait. It is generally accepted that changes in ice sheet dynamics were involved in the MPT (for review see *Clark et al.* [2006]). For example, *Clark and Pollard* [1998] proposed the "regolith hypothesis" to explain the MPT, whereby progressive glacial erosion of regolith and exposure of bedrock changed the basal boundary conditions of the LIS from an all soft-bedded to a mixed hard-soft bedded layer. Prior to 650 ka, the LIS was thinner and responded linearly to 41-ka insolation forcing [*Clark et al.*, 2006]. Erosion of regolith and exposure of high-friction crystalline basement permitted the development of a thicker LIS that, in turn, may have introduced LIS instability manifest by ice mass fluctuations (e.g., Heinrich events).

[31] The observation that HS Heinrich layers were absent at Site U1308 prior to 640 ka does not necessarily mean that ice sheets were less variable during the 41-ka world. Detrital carbonate layers only reflect specific dynamical glacial

processes of the LIS in the region of Hudson Strait. In fact, Si-rich IRD events appear to be more frequent during the 41-ka world prior to 640 ka than afterward. *Raymo et al.* [1998] also provided clear evidence for millennial-scale climate variability in IRD during MIS 40 and 44 at Site 983 in the North Atlantic, indicating that millennial-scale variations in iceberg discharge were occurring during the 41-ka world. Other studies have suggested that millennial-scale variability increased across the MPT as the size of Northern Hemisphere ice sheets expanded [*Larrasoana et al.*, 2003; *Weirauch et al.*, 2008].

4.3. Comparison of Deep and Surface Water Proxies

[32] The leading hypothesis to explain millennial-scale oscillations in the North Atlantic during the last glaciation involves changes in the strength of thermohaline circulation (for review, see *Alley* [2007]). Instability of Northern Hemisphere ice sheets results in enhanced production of icebergs to the North Atlantic. The meltwater produced from these abundant icebergs decreases sea surface salinity and increases surface water stratification and stability of the water column. This process acts as a positive feedback to cooling by both increasing sea ice formation (thereby increasing albedo) and diminishing rates of thermohaline circulation. This hypothesis predicts a strong coupling between North Atlantic surface and deep water proxies.

[33] Site U1308 is located in 3872m water depth and is bathed today by North East Atlantic Deep Water, which consists of ~30% Iceland-Scotland Overflow Water (ISOW), 45% Labrador Sea Water, and 23% Lower Deep Water (LDW) [*van Aken*, 2000]. During the last glaciation, the site was more influenced by LDW of Southern Ocean origin [*Curry and Oppo*, 2005]. Consequently, the Site U1308 benthic $\delta^{13}C$ record is sensitive to changes in the mixing ratio between northern and southern sourced waters. DSDP Site 607 (3427 m water depth) has traditionally served as a benthic $\delta^{13}C$ reference section for the deep North Atlantic to which other records are compared [*Raymo et al.*, 2004]. The glacial-to-interglacial changes in $\delta^{13}C$ are virtually identical between Site U1308 and Site 607, but the higher-resolution data at Site U1308 also records millennial-scale changes in benthic $\delta^{13}C$.

[34] We observe a tight coupling between Si/Sr and benthic $\delta^{13}C$ variation at Site U1308 on glacial-interglacial time scales during the Pleistocene (Figure 10a). This relationship also extends to millennial time scales as each of the major peaks in Si/Sr at Site U1308 coincides with a minimum in benthic $\delta^{13}C$ for the past 100 ka (Figure 10b). Si/Sr peaks reflect a low in carbonate productivity and/or an increase in silicate-rich IRD, presumably reflecting iceberg melting and low salinity. The tight coupling of benthic $\delta^{13}C$ and Si/Sr at Site U1308 supports previous findings of a strong link between iceberg discharge, lowered salinity, and weakening of thermohaline circulation. Alternatively, the reduction in Atlantic meridional overturning circulation itself might have induced an IRD event either through an ice sheet mass balance response or ice shelf collapse [*Clark et al.*, 2007].

5. Conclusions

[35] We found that Ca/Sr of bulk sediment provides a rapid, nondestructive method for identifying layers that are rich in detrital carbonate and poor in biogenic carbonate (i.e., cemented marl–type or HS Heinrich layers) at Site U1308 in the IRD belt of the North Atlantic. In addition to Heinrich events 1, 2, 4 and 5 of the last glaciation, detrital carbonate layers were recognized in MIS 8, 10, 12 and 16, but were absent from MIS 6 and 14 and in glacial periods prior to ~640 ka. HS Heinrich events generally occur late in the glacial stage and very often at glacial terminations. HS Heinrich layers first appeared in the sedimentary record of Site U1308 at ~640 ka during MIS 16, coincident with an increase in 100-ka power in the benthic $\delta^{18}O$ record. Although we cannot rule out that SST or surface circulation played a role in affecting iceberg survivability or transport, we favor a production explanation for the abrupt onset of HS Heinrich layers near the end of the MPT. We speculate that ice volume (i.e., thickness) and duration of glacial conditions surpassed a critical threshold during MIS 16 and activated the dynamical processes responsible for LIS instability in the region of Hudson Strait. Prior to MIS 16, ice sheets were reduced in thickness and the duration of glacial periods may have been too short for a substantial fraction of the LIS to reach the pressure melting point.

[36] Si/Sr provides a proxy for IRD layers that are rich in detrital silicate minerals and poor in biogenic carbonate. Si/Sr peaks are more common than detrital carbonate events and reflect different sources and/or glaciological processes than Heinrich layers. A major change occurred in both the composition and frequency of IRD delivery to Site U1308 during the MPT. Prior to 640 ka (MIS 16), IRD events were rich in silicates (quartz) and frequency was strongly dominated by 41-ka cyclicity. After 640 ka, Si/Sr was dominated by the 100-ka cycle and detrital carbonate derived from Hudson Strait appeared in the IRD. These changes support previous findings implicating changes in the volume and dynamics of Northern Hemisphere ice sheets as an important process for the MPT. A tight coupling is observed between iceberg discharge (Si/Sr) and benthic $\delta^{13}C$ for the last 1.4 Ma, supporting a strong coupling between freshwater fluxes to the North Atlantic and thermohaline circulation.

[37] **Acknowledgments.** We thank G. Browne for preparation of samples for stable isotope analysis, V. Lukies and H. Pfletschinger for technical assistance with scanning XRF, and A. Wuelbers and W. Hale for their help at the Bremen Core Repository. P. Clark and two anonymous reviewers provided insightful suggestions that significantly improved the manuscript. This research used samples provided by the Integrated Ocean Drilling Program (IODP). Funding for this research was provided by the Joint Oceanographic Institutions–United States Science Support Program.

References

Alley, R. B. (2007), Wally was right: Predictive ability of the North Atlantic "conveyor belt" hypothesis for abrupt climate change, *Annu. Rev. Earth Planet. Sci.*, *35*, 241–272, doi:10.1146/annurev.earth.35.081006.131524.

Alley, R. B., and P. U. Clark (1999), The deglaciation of the northern hemisphere: A global perspective, *Annu. Rev. Earth Planet. Sci.*, *27*, 149–182, doi:10.1146/annurev.earth.27.1.149.

Alley, R. B., and D. R. MacAyeal (1994), Ice-rafted debris associated with binge/purge oscil-

lations of the Laurentide Ice Sheet, *Paleoceanography*, *9*, 503–512, doi:10.1029/94PA01008.

Andrews, J. T. (1998), Abrupt changes (Heinrich events) in late Quaternary North Atlantic marine environments: A history and review of data and concepts, *J. Quat. Sci.*, *13*, 3–16, doi:10.1002/(SICI)1099-1417(199801/02)13:1<3::AID-JQS361>3.0.CO;2-0.

Andrews, J. T., and K. Tedesco (1992), Detrital carbonate-rich sediments, northwestern Labrador Sea: Implications for ice-sheet dynamics and iceberg rafting (Heinrich) events in the North Atlantic, *Geology*, *20*, 1087–1090, doi:10.1130/0091-7613(1992)020<1087:DCRSNL>2.3.CO;2.

Andrews, J. T., A. E. Jennings, M. Kerwin, M. Kirby, W. Manley, and G. H. Miller (1995), A Heinrich-like event, H-0 (DC-0): Source (s) for detrital carbonate in the North Atlantic during the Younger Dryas chronozone, *Paleoceanography*, *10*, 943–952, doi:10.1029/95PA01426.

Berger, W. H., and E. Jansen (1994), Mid-Pleistocene climate shift: The Nansen connection, in *The Polar Oceans and Their Role in Shaping the Global Environment*, *Geophys. Monogr. Ser.*, vol. 84, edited by O. M. Johannessen, R. D. Muench, and J. E. Overalnd, pp. 295–311, AGU, Washington, D. C.

Bond, G. C., and R. Lotti (1995), Iceberg discharges into the North Atlantic on millennial time scales during the last glaciation, *Science*, *267*, 1005–1010, doi:10.1126/science.267.5200.1005.

Bond, G., et al. (1992), Evidence for massive discharges of icebergs into the North Atlantic Ocean during the last glacial period, *Nature*, *360*, 245–249, doi:10.1038/360245a0.

Bond, G., W. Broecker, S. Johnsen, J. McManus, L. Labeyrie, J. Jouzel, and G. Bonani (1993), Correlations between climate records from North Atlantic sediments and Greenland ice, *Nature*, *365*, 143–147, doi:10.1038/365143a0.

Bond, G. C., W. Showers, M. Elliot, M. Evans, R. Lotti, I. Hajdas, G. Bonani, and S. Johnson (1999), The North Atlantic's 1–2 kyr climate rhythm: Relation to Heinrich events, Dansgaard/Oeschger cycles and the Little Ice Age, in *Mechanisms of Global Climate Change at Millennial Time Scales*, *Geophys. Monogr. Ser.*, vol. 112, edited by P. U. Clark, R. S. Webb, and L. D. Keigwin, pp. 35–58, AGU, Washington, D. C.

Broecker, W. S., G. Bond, M. Klas, E. Clark, and J. McManus (1992), Origin of the northern Atlantic's Heinrich events, *Clim. Dyn.*, *6*, 265–273, doi:10.1007/BF00193540.

Calvo, E., J. Villanueva, J. O. Grimalt, A. Boelaert, and L. Labeyrie (2001), New insights into the glacial latitudinal temperature gradients in the North Atlantic. Results from U^{K}_{37} sea surface temperatures and terrigenous inputs, *Earth Planet. Sci. Lett.*, *188*, 509–519, doi:10.1016/S0012-821X(01)00316-8.

Channell, J. E. T., D. A. Hodell, C. Xuan, A. Mazaud, and J. S. Stoner (2008), Age calibrated relative paleointensity for the last 1.5 Myr at IODP Site U1308 (North Atlantic), *Earth Planet. Sci. Lett.*, *134*, 59–71.

Chapman, M. R., and N. J. Shackleton (1998), Millennial-scale fluctuations in North Atlantic heat flux during the last 150,000 years, *Earth Planet. Sci. Lett.*, *159*, 57–70, doi:10.1016/S0012-821X(98)00068-5.

Chapman, M. R., and N. J. Shackleton (1999), Global ice-volume fluctuations, North Atlantic ice-rafting events, and deep-ocean circulation changes between 130 and 70 ka, *Geology*, *27*, 795–798, doi:10.1130/0091-7613(1999)027<0795:GIVFNA>2.3.CO;2.

Clark, P. U., and D. Pollard (1998), Origin of the middle Pleistocene transition by ice sheet erosion of regolith, *Paleoceanography*, *13*, 1–9, doi:10.1029/97PA02660.

Clark, P. U., D. Archer, D. Pollard, J. D. Blum, J. A. Rial, V. Brovkin, A. C. Mix, N. G. Pisias, and M. Roy (2006), The middle Pleistocene transition: Characteristics, mechanisms, and implications for long-term changes in atmospheric CO_2, *Quat. Sci. Rev.*, *25*, 3150–3184, doi:10.1016/j.quascirev.2006.07.008.

Clark, P. U., S. W. Hostetler, N. G. Pisias, A. Schmittner, and K. J. Meissner (2007), Mechanisms for an ~7-kyr climate and sea-level oscillation during marine isotope stage 3, in *Ocean Circulation: Mechanisms and Impacts*, *Geophys. Monogr. Ser.*, vol. 173, edited by A. Schmittner et al., pp. 209–246, AGU, Washington, D. C.

Clarke, G. K. C., D. W. Leverington, J. T. Teller, A. S. Dyke, and S. J. Marshall (2005), Fresh arguments against the Shaw megaflood hypothesis. A reply to comments by David Sharpe on "Paleohydraulics of the last outburst flood from glacial Lake Agassiz and the 8200 BP cold event", *Quat. Sci. Rev.*, *24*, 1533–1541, doi:10.1016/j.quascirev.2004.12.003.

Curry, W. B., and D. W. Oppo (2005), Glacial water mass geometry and the distribution of $\delta^{13}C$ of ΣCO_2 in the western Atlantic Ocean, *Paleoceanography*, *20*, PA1017, doi:10.1029/2004PA001021.

de Abreu, L., N. J. Shackleton, J. Schonfeld, M. Hall, and M. Chapman (2003), Millennial-scale oceanic climate variability off the western Iberian margin during the last two glacial periods, *Mar. Geol.*, *196*, 1–20.

Elliot, M., L. Labeyrie, G. Bond, E. Cortijo, J. L. Turon, N. Tisnerat, and J. C. Duplessy (1998), Millennial-scale iceberg discharges in the Irminger Basin during the last glacial period: Relationship with the Heinrich events and environmental settings, *Paleoceanography*, *13*, 433–446, doi:10.1029/98PA01792.

Expedition 303 Scientists (2006), Site U1308, *Proc. Integrated Ocean Drill. Program*, *303*, 1–98, doi:10.2204/iodp.proc.303306.108.2006.

Grousset, F. E., L. Labeyrie, J. A. Sinko, M. Cremer, G. Bond, J. Duprat, E. Cortijo, and S. Huon (1993), Patterns of ice-rafted detritus in the glacial North Atlantic (40–55°N), *Paleoceanography*, *8*, 175–192, doi:10.1029/92PA02923.

Gwiazda, R. H., S. R. Hemming, and W. S. Broecker (1996), Provenance of icebergs during Heinrich event 3 and the contrast to their sources during other Heinrich episodes, *Paleoceanography*, *11*, 371–378, doi:10.1029/96PA01022.

Heinrich, H. (1988), Origin and consequences of cyclic ice rafting in the northeast Atlantic Ocean during the past 130,000 years, *Quat. Res.*, *29*, 142–152, doi:10.1016/0033-5894(88)90057-9.

Hemming, S. R. (2004), Heinrich events: Massive late Pleistocene detritus layers of the North Atlantic and their global climate imprint, *Rev. Geophys.*, *42*, RG1005, doi:10.1029/2003RG000128.

Hemming, S. R., W. S. Broecker, W. D. Sharp, G. C. Bond, R. H. Gwiazda, J. F. McManus, M. Klas, and I. Hajdas (1998), Provenance of the Heinrich layers in core V28–82, northeastern Atlantic: ^{40}Ar-^{39}Ar ages of ice-rafted hornblende, Pb isotopes in feldspar grains, and Nd-Sr-Pb isotopes in the fine sediment fraction, *Earth Planet. Sci. Lett.*, *164*, 317–333, doi:10.1016/S0012-821X(98)00224-6.

Hesse, R., H. Rashid, and S. Khodabakhsh (2004), Fine-grained sediment lofting from meltwater-generated turbidity currents during Heinrich events, *Geology*, *32*, 449–452, doi:10.1130/G20136.1.

Hillaire-Marcel, C., A. de Vernal, G. Bilodeau, and G. Wu (1994), Isotope stratigraphy, sedimentation rates, deep circulation, and carbonate events in the Labrador Sea during the last ~200 ka, *Can. J. Earth Sci.*, *31*, 68–89.

Hiscott, R. N., A. E. Aksu, P. J. Mudie, and D. F. Parsons (2001), A 340,000 year record of ice rafting, palaeoclimatic fluctuations, and shelf-crossing glacial advances in the southwestern Labrador Sea, *Global Planet. Change*, *28*, 227–240, doi:10.1016/S0921-8181(00)00075-8.

Hodell, D. A., and J. H. Curtis (2008), Oxygen and carbon isotopes of detrital carbonate in North Atlantic Heinrich events, *Mar. Geol.*, *256*, 30–35, doi:10.1016/j.margeo.2008.09.010.

Hulbe, C. L. (1997), An ice shelf mechanism for Heinrich layer production, *Paleoceanography*, *12*, 711–717, doi:10.1029/97PA02014.

Hulbe, C. L., D. R. MacAyeal, G. H. Denton, J. Kleman, and T. V. Lowell (2004), Catastrophic ice shelf breakup as the source of Heinrich event icebergs, *Paleoceanography*, *19*, PA1004, doi:10.1029/2003PA000890.

Ji, J., G. Yun, W. Balsam, J. E. Damuth, and J. Chen (2008), Rapid identification of dolomite using a Fourier transform infrared spectrophotometer (FTIR): A fast method for identifying Heinrich events in IODP Site U1308, *Mar. Geol.*, in press.

Kissel, C. (2005), Magnetic signature of rapid climatic variations in glacial North Atlantic, a review, *C. R. Geosci.*, *337*, 908–918, doi:10.1016/j.crte.2005.04.009.

Larrasoana, J. C., A. P. Roberts, E. J. Rohling, M. Winklhofer, and R. Wehausen (2003), Three million years of monsoon variability over the northern Sahara, *Clim. Dyn.*, *21*, 689–698, doi:10.1007/s00382-003-0355-z.

Lisiecki, L. E., and M. E. Raymo (2005), A Pliocene-Pleistocene stack of 57 globally distributed benthic $\delta^{18}O$ records, *Paleoceanography*, *20*, PA1003, doi:10.1029/2004PA001071.

Lototskaya, A., and G. M. Ganssen (1999), The structure of Termination II (penultimate deglaciation and Eemian) in the North Atlantic, *Quat. Sci. Rev.*, *18*, 1641–1654, doi:10.1016/S0277-3791(99)00011-6.

MacAyeal, D. R. (1993a), A low-order model of growth/purge oscillations of the Laurentide Ice Sheet, *Paleoceanography*, *8*, 767–773, doi:10.1029/93PA02201.

MacAyeal, D. R. (1993b), Binge/purge oscillations of the Laurentide Ice Sheet as a cause of the North Atlantic Heinrich events, *Paleoceanography*, *8*, 775–784, doi:10.1029/93PA02200.

Marshall, S. J., and P. U. Clark (2002), Basal temperature evolution of North American ice sheets and implications for the 100-kyr cycle, *Geophys. Res. Lett.*, *29*(24), 2214, doi:10.1029/2002GL015192.

Marshall, S. J., and M. R. Koutnik (2006), Ice sheet action versus reaction: Distinguishing between Heinrich events and Dansgaard-Oeschger cycles in the North Atlantic, *Paleoceanography*, *21*, PA2021, doi:10.1029/2005PA001247.

Martrat, B., J. O. Grimalt, C. Lopez-Martinez, I. Cacho, F. J. Sierro, J. A. Flores, R. Zahn, M. Canals, J. H. Curtis, and D. A. Hodell (2004), Abrupt temperature changes in the western Mediterranean over the last 250,000 years, *Science*, *306*, 1762–1765, doi:10.1126/science.1101706.

Martrat, B., J. O. Grimalt, N. J. Shackleton, L. de Abreu, M. A. Hutterli, and T. F. Stocker (2007), Four climate cycles of recurring deep and surface water destabilizations on the Iberian Margin, *Science*, *317*, 502–507, doi:10.1126/science.1139994.

McManus, J. F., G. C. Bond, W. S. Broecker, S. Johnsen, L. Labeyrie, and S. Higgins (1994), High-resolution climate records from the North Atlantic during the last interglacial, *Nature*, *371*, 326–329, doi:10.1038/371326a0.

McManus, J. F., R. F. Anderson, W. S. Broecker, M. Q. Fleisher, and S. M. Higgins (1998), Radiometrically determined sedimentary fluxes in the sub-polar North Atlantic during the last 140,000 years, *Earth Planet. Sci. Lett.*, *155*, 29–43, doi:10.1016/S0012-821X(97)00201-X.

Mudelsee, M., and M. Schulz (1997), The Mid-Pleistocene climate transition: Onset of 100 ka cycle lags ice volume buildup by 280 ka, *Earth Planet. Sci. Lett.*, *151*, 117–123, doi:10.1016/S0012-821X(97)00114-3.

Mudelsee, M., and K. Stattegger (1997), Exploring the structure of the mid-Pleistocene revolution with advanced methods of time-series analysis, *Geol. Rundsch.*, *86*, 499–511, doi:10.1007/s005310050157.

Oppo, D. W., L. D. Keigwin, and J. F. McManus (2001), Persistent suborbital climate variability in marine isotope stage 5 and Termination II, *Paleoceanography*, *16*, 280–292, doi:10.1029/2000PA000527.

Oppo, D. W., J. F. McManus, and J. L. Cullen (2006), Evolution and demise of the last interglacial warmth in the subpolar North Atlantic, *Quat. Sci. Rev.*, *25*, 3268–3277, doi:10.1016/j.quascirev.2006.07.006.

Peck, V. L., I. R. Hall, R. Zahn, and J. D. Scourse (2007), Progressive reduction in NE Atlantic intermediate water ventilation prior to Heinrich events: Response to NW European ice sheet instabilities?, *Geochem. Geophys. Geosyst.*, *8*, Q01N10, doi:10.1029/2006GC001321.

Rashid, H., R. Hesse, and D. J. W. Piper (2003a), Evidence for an additional Heinrich event between H5 and H6 in the Labrador Sea, *Paleoceanography*, *18*(4), 1077, doi:10.1029/2003PA000913.

Rashid, H., R. Hesse, and D. J. W. Piper (2003b), Distribution, thickness and origin of Heinrich layer 3 in the Labrador Sea, *Earth Planet. Sci. Lett.*, *205*, 281–293, doi:10.1016/S0012-821X(02)01047-6.

Raymo, M. E., K. Ganley, S. Carter, D. W. Oppo, and J. McManus (1998), Millennial-scale climate instability during the early Pleistocene epoch, *Nature*, *392*, 699–702, doi:10.1038/33658.

Raymo, M. E., D. Oppo, B. P. Flower, D. A. Hodell, J. F. McManus, K. A. Venz, K. F. Kleiven, and K. McIntyre (2004), Stability of North Atlantic water masses in face of pronounced climate variability during the Pleistocene, *Paleoceanography*, *19*, PA2008, doi:10.1029/2003PA000921.

Richter, T. O., S. van der Gaast, B. Koster, A. Vaars, R. Gieles, H. C. de Stigter, H. de Haas, and T. C. E. van Weering (2006), The Avaatech XRF Core Scanner: Technical description and applications to NE Atlantic sediments, in *New Techniques in Sediment Core Analysis*, edited by G. Rothwell, *Spec. Publ. Geol. Soc.*, *267*, 39–50.

Robinson, S. G., M. A. Maslin, and N. McCave (1995), Magnetic susceptibility variations in upper Pleistocene deep-sea sediments of the NE Atlantic: Implications for ice rafting and paleocirculation at the Last Glacial Maximum, *Paleoceanography*, *10*, 221–250, doi:10.1029/94PA02683.

Romero, O. E., and D. A. Hodell (2007), High-resolution climatic record of the high-latitude Atlantic (Site 1302/03, IODP Exp 303): Pleistocene occurrence of rapidly-deposited detrital layers, *Geophys. Res. Abstr.*, *9*, 08311.

Ruddiman, W. F. (1977), Late Quaternary deposition of ice-rafted sand in the subpolar North Atlantic (lat 40° to 65°N), *Geol. Soc. Am. Bull.*, *88*, 1813–1827, doi:10.1130/0016-7606(1977)88<1813:LQDOIS>2.0.CO;2.

Ruddiman, W., M. Raymo, D. Martinson, B. Clement, and J. Backman (1989), Pleistocene evolution: Northern Hemisphere ice sheets and North Atlantic Ocean, *Paleoceanography*, *4*, 353–412, doi:10.1029/PA004i004p00353.

Scourse, J. D., I. R. Hall, I. N. McCave, J. R. Young, and C. Sugdon (2000), The origin of Heinrich layers: Evidence from H2 for European precursor events, *Earth Planet. Sci. Lett.*, *182*, 187–195, doi:10.1016/S0012-821X(00)00241-7.

Shackleton, N. J., R. G. Fairbanks, T.-C. Chiu, and F. Parrenin (2004), Absolute calibration of the Greenland time scale: Implications for Antarctic time scales and for $\Delta^{14}C$, *Quat. Sci. Rev.*, *23*, 1513–1522, doi:10.1016/j.quascirev.2004.03.006.

Snoeckx, H., F. Grousset, M. Revel, and A. Boelaert (1999), European contribution of ice-rafted sand to Heinrich layers H3 and H4, *Mar. Geol.*, *158*, 197–208, doi:10.1016/S0025-3227(98)00168-6.

Stoner, J. S., and J. T. Andrews (1999), The North Atlantic as a Quaternary magnetic archive, in *Quaternary Climates, Environments and Magnetism*, edited by B. Maher and R. Thompson, pp. 49–80, Cambridge Univ. Press, Cambridge, U. K.

Stoner, J. S., J. E. T. Channell, and C. Hillaire-Marcel (1995), Late Pleistocene relative geomagnetic paleointensity from the deep Labrador Sea: Regional and global correlations, *Earth Planet. Sci. Lett.*, *134*, 237–252, doi:10.1016/0012-821X(95)00134-X.

Stoner, J. S., J. E. T. Channell, and C. Hillaire-Marcel (1996), The magnetic signature of rapidly deposited detrital layers from the deep Labrador Sea: Relationship to North Atlantic Heinrich layers, *Paleoceanography*, *11*, 309–325, doi:10.1029/96PA00583.

Stoner, J. S., J. E. T. Channell, and C. Hillaire-Marcel (1998), A 200 ka geomagnetic chronostratigraphy for the Labrador Sea: Indirect correlation of the sediment record to SPECMAP, *Earth Planet. Sci. Lett.*, *159*, 165–181, doi:10.1016/S0012-821X(98)00069-7.

Stoner, J. S., J. E. T. Channell, C. Hillaire-Marcel, and C. Kissel (2000), Geomagnetic paleointensity and environmental record from Labrador Sea core MD95–2024: Global marine sediment and ice core chronostratigraphy for the last 110 kyr, *Earth Planet. Sci. Lett.*, *183*, 161–177, doi:10.1016/S0012-821X(00)00272-7.

Svensson, A., et al. (2006), The Greenland Ice Core Chronology 2005, 15–42 ka, part. 2: Comparison to other records, *Quat. Sci. Rev.*, *25*, 3258–3267, doi:10.1016/j.quascirev.2006.08.003.

Tauxe, L., J. L. LaBrecque, D. Dodson, and M. Fuller (1983), U-channels: A new technique for paleomagnetic analysis of hydraulic piston cores, *Eos Trans. AGU*, *64*, 219.

Thomas, R. G., Y. Guyodo, and J. E. T. Channell (2003), U channel track for susceptibility measurements, *Geochem. Geophys. Geosyst.*, *4*(6), 1050, doi:10.1029/2002GC000454.

Tjallingii, R., U. Roehl, M. Koelling, and T. Bickert (2007), Influence of the water content on X-ray fluorescence core-scanning measurements in soft marine sediments, *Geochem. Geophys. Geosyst.*, *8*, Q02004, doi:10.1029/2006GC001393.

van Aken, H. M. (2000), The hydrography of the mid-latitude Northeast Atlantic Ocean—Part I: The deep water masses, *Deep Sea Res., Part I*, *47*, 757–788, doi:10.1016/S0967-0637(99)00092-8.

van Kreveld, S. A., M. Knappertsbusch, J. Ottens, G. M. Ganssen, and J. E. van Hinte (1996), Biogenic carbonate and ice-rafted debris (Heinrich layer) accumulation in deep-sea sediments from a northeast Atlantic piston core, *Mar. Geol.*, *131*, 21–46, doi:10.1016/0025-3227(95)00143-3.

Venz, K. A., D. A. Hodell, C. Stanton, and D. A. Warnke (1999), A 1.0 Ma record of Glacial North Atlantic Intermediate Water variability from ODP Site 982 in the northeast Atlantic, *Paleoceanography*, *14*, 42–52, doi:10.1029/1998PA900013.

Walden, J., E. Wadsworth, W. E. N. Austin, C. Peters, J. D. Scourse, and I. R. Hall (2006), Compositional variability of ice-rafted debris in Heinrich layers 1 and 2 on the northwest European continental slope identified by environmental magnetic analyses, *J. Quat. Sci.*, *22*, 163–172, doi:10.1002/jqs.1020.

Weirauch, D., K. Billups, and P. Martin (2008), Evolution of millennial-scale climate variability during the mid-Pleistocene, *Paleoceanography*, *23*, PA3216, doi:10.1029/2007PA001584.

Wien, K., D. Wissmann, K. Martin, and H. D. Schulz (2005), Fast application of X-ray fluorescence spectrometry aboard ship: How good is the new portable Spectro Xepos analyser?, *Geo-Mar. Lett.*, *25*, 248–264, doi:10.1007/s00367-004-0206-x.

Wright, A. K., and B. P. Flower (2002), Surface and deep ocean circulation in the subpolar North Atlantic during the mid-Pleistocene revolution, *Paleoceanography*, *17*(4), 1068, doi:10.1029/2002PA000782.

J. E. T. Channell and J. H. Curtis, Department of Geological Sciences, University of Florida, P.O. Box 112120, Gainesville, FL 32611, USA.

D. A. Hodell, Godwin Laboratory for Paleoclimate Research, Department of Earth Sciences, University of Cambridge, Downing Street, Cambridge CB2 3EQ, UK. (dhod07@esc.cam.ac.uk)

U. Röhl, Center for Marine Environmental Research, University of Bremen, Leobener Strasse, Bremen D-28359, Germany.

O. E. Romero, Instituto Andaluz de Ciencias de la Tierra, Universidad de Granada, E-18002 Granada, Spain.